On the Description of the Orientation State for Fiber Suspensions in Homogeneous Flows

M. C. ALTAN, S. G. ADVANI, S. I. GÜÇERI, and R. B. PIPES,
Center for Composite Materials and Department of Mechanical Engineering, University of Delaware, Newark, Delaware 19716

Synopsis

This work investigates the two- and three-dimensional description of fiber orientation in homogeneous flow fields. Motion of the fibers is described using the Dinh–Armstrong model which was developed for semiconcentrated fiber suspensions. The calculation of rheological properties for fiber suspensions requires the determination of fourth-order moments of orientation distribution function which is defined as the fourth-order orientation tensor. Solution of the distribution function is obtained in terms of the velocity gradients and transient calculations are presented for simple shear, planar elongational, and uniaxial extensional flows. Second- and fourth-order tensors are calculated by using the distribution function and the components of the second-order tensor are utilized to define an orientation ellipsoid for the graphical representation of the orientation state. The fourth-order tensor is approximated from second-order tensors through quadratic and hybrid closure equations, and compared with the exact results. Despite the qualitative agreement between the exact and approximated results, considerable quantitative discrepancy is observed which may result in inaccurate prediction of suspension behavior.

INTRODUCTION

The characterization of the flow or the fiber orientation in a short fiber suspension is a major concern in current polymer processing research. Short fiber suspensions are commonly used in such manufacturing techniques as extrusion, injection, and compression molding. During these processes, fibers being affected by the flow regime inside the mold, form a flow-induced orientation state leading to an anisotropic product. In order to perform a proper design, the description of the anisotropy and the ways to control it must be well understood.

Several studies have characterized the orientation state in fiber suspension systems. Jeffery's[1] early work on the motion of an ellipsoid in a viscous Newtonian fluid was used by Givler et al.,[2] and a computer code was developed to predict the orientation angle in dilute suspensions in confined geometries.

Journal of Rheology, 33(7), 1129–1155 (1989) CCC 0148-6055/89/071129-27$04.00

The last decade has seen additional activity in the development of reliable models to characterize the behavior of nondilute fiber suspensions. Folgar and Tucker[3] have proposed a phenomenological model which incorporates the effects of the interaction among rigid fibers. In this model the description of fiber orientation is described by using an orientation distribution function. Later, Advani and Tucker[4] used orientation tensors to describe the orientation.

Dinh and Armstrong[5] have developed a rheological model for semiconcentrated suspensions, in which a constitutive equation which requires the calculation of the fourth-order moments of the distribution function is proposed to calculate the rheological properties. Experiments performed by Bibbo et al.[6] have shown good agreement with the theoretical predictions in simple shear flow.

All of these proposed models for fiber suspensions require some form of description of the fiber orientation. The simplest case is the use of a scalar, which is usually the angle θ between the fiber axis and one of the reference axes. For three-dimensional cases, both θ and ϕ must be used to specify the orientation angle in spherical coordinates.[3]

However, this representation is not suitable for the determination of rheological properties; instead, at a given point and time, the orientation distribution function for fibers provides a complete description of the orientation state.[7] There have been several studies on the solution of the orientation distribution function. The governing equation is a linear PDE and is also known as the Fokker–Planck equation. If the particles in the suspension are small enough to consider the Brownian effects, the analytical solution is not available. Leal and Hinch[8] analyzed the effect of weak Brownian rotations on the fiber orientation distribution for simple shear flows. Okagawa et al.,[9] assuming negligible Brownian diffusion, gave the analytical solution for distribution function for simple shear flows. Strand et al.[10] solved the distribution function by using spectral methods. They considered the Brownian effects for an infinite fiber aspect ratio for simple shear flows. Although orientation distribution function contains the complete description, it is not always necessary to make use of this function. More compact forms of representations are possible by defining the moments of the distribution function as orientation tensors, which are also widely used in short fiber composites,[11] semicrystalline polymers,[12] and polymeric liquid crystals,[13,14] and have an advantage over the tedious calculation of the distribution function. Several of these rheological models employ second- and fourth-order orientation tensors.[5,13,15] In most of the applications of these models, as an alternative to calculating the orientation tensors by integrating over the distribution function, the rate of change of the orientation tensors is obtained by the proper integration of the Fokker–Plank equation. However, the resulting set of equations exhibits the classical closure problem where the higher-order orientation tensors have to be approximated from the lower order ones. Common practice is to estimate the fourth-order tensor by using second-order orientation tensor components.[16–18] Several different closure schemes are available (i.e., quadratic, linear, hybrid); however, the error caused by these closure approximations must be carefully investigated and the suitable order and type of approximation should be used.

The Dinh–Armstrong model and the basics of orientation distribution function are briefly presented below. The subsequent section illustrates how the solution of distribution function is obtained in terms of flow kinematics. The solutions are derived for any two-dimensional and for a particular class of three-dimensional ($u_1 = f_1(x_1, x_2, x_3)$, $u_2 = f_2(x_1, x_2, x_3)$, $u_3 = 0$) homogeneous flows. Next, the commonly used rheological parameters are expressed in terms of the fourth-order orientation tensor components and the tensorial approximations are introduced. In the final section, the accuracy of closure approximations is investigated by computing the exact and approximate rheological properties and fourth-order tensor components for simple shear and planar elongational flows.

THEORY

Dinh-Armstrong Model

In developing a fundamental model for fiber orientation, a structural model can provide a direct link between the microstructural properties and the macroscopic rheological behavior of a suspension system. Therefore, the ambiguities encountered in the phenomenological models are avoided. Instead, the results from a structural study can be used to establish the proper form of the continuum models. In semiconcentrated regions, the subject of the current study, the average spacing between the fibers varies from its diameter to its length. The effect of the orientation state of fibers should be included in the constitutive equation in order to describe the system completely. The suspension may evidently be regarded as a homogeneous fluid if the length scale of the motion imposed on the suspension is large compared with the average spacing between particles. Therefore, the problem is to find the rheological characteristics from the constituents, namely fiber and the fluid.

The bulk stresses generated in the suspensions can be assumed to have two separate parts, one due to the viscous dissipation of the fluid and the other due to the presence of particles.[19] A suitably chosen volume V is used in the analysis which is large enough to contain many fibers but small enough to neglect the variation of the velocity gradient. Thus, a homogeneous flow is required within volume V. Additionally, assuming rigid fibers and using no-slip boundary condition on the fiber surface, the stress tensor $\boldsymbol{\sigma}_{ij}^{(p)}$ generated in the homogeneous flow fields due to the presence of particles can be expressed as:[5]

$$\boldsymbol{\sigma}_{ij}^{(p)} = \mu \frac{\pi l^3 n}{6 \ln\left(\frac{2H}{d}\right)} \int u_{k,l} p_k p_l p_i p_j \psi(\mathbf{p}, t)\, d\mathbf{p} \tag{1}$$

where

n = number density of suspension
l = fiber length
d = fiber diameter
$u_{k,l} = \frac{\partial u_k}{\partial x_l}$; components of the velocity gradient tensor
p_i = i-th component of the unit vector denoting the fiber orientation
$\psi(\mathbf{p}, t)$ = distribution function for the fiber orientation
H = average distance from a given fiber to its nearest neighbor
$= (nl)^{-1/2}$ for aligned systems
$= (nl^2)^{-1}$ for random systems
μ = absolute viscosity of the fluid

In this expression,* fibers are taken as line elements, and a self-consistent continuum approach is made on a representative test fiber which is assumed to be immersed in an effective medium. This effective medium is considered to be the continuum approximation of the effect of the other fibers.

*Cartesian tensor notation is used throughout the text and summation over the repeated indices is implied.

With the assumptions stated before, the extra stress tensor due to the fibers $\sigma_{ij}^{(p)}$ can be written in the form:

$$\sigma_{ij}^{(p)} = \mu \frac{\pi l^3 n}{6 \ln\left(\frac{2H}{d}\right)} u_{k,l} S_{ijkl} \tag{2}$$

where S_{ijkl} is the fourth moment of the distribution function and defined as the fourth-order orientation tensor. The equation of motion for the fibers can be expressed in the form of Jeffery's equation with infinite fiber aspect ratio,

$$\dot{p}_i = u_{i,q} p_q - u_{k,q} p_q p_k p_i \tag{3}$$

Equation (3) is already built in Eq. (2) and the coefficient of the integral in Eq. (1) is determined by using the structural analysis of semiconcentrated suspensions.[19]

Orientation Distribution Function

The orientation distribution function $\psi(\mathbf{p}, t)$, which gives the probability of having a fiber with an orientation $\mathbf{p}$ at time t, is the most basic and complete description of the fiber orientation state. The orientation distribution function can be defined for both two- (planar) and three-dimensional cases. If all fibers are known to lie in a single plane, then a planar distribution function is sufficient to describe the orientation state.

For two-dimensional descriptions, the distribution function has a period of π,

$$\psi_\theta(\theta) = \psi_9(\theta + \pi) \tag{4}$$

The normalization condition implies that the integration over all the possible orientations must be unity:

$$\int_0^\pi \psi_\theta(\theta)\, d\theta = 1 \tag{5}$$

For three-dimensional cases all possible orientations constitute a unit sphere. Hence, for three-dimensional orientations, Eq. (4) can be written as

$$\psi(\theta, \phi) = \psi(\pi - \theta, \phi + \pi) \tag{6}$$

and the normalization condition becomes,

$$\int_0^{2\pi} \int_0^\pi \psi(\theta, \phi) \sin\theta\, d\theta\, d\phi = 1 \tag{7}$$

The governing equation for $\psi(\mathbf{p}, t)$ depends on the conservation of fiber orientation. This is, in a sense, the continuity condition for the distribution function. For homogeneous flow fields with negligible Brownian rotation, it is given by:

$$\frac{\partial\psi(\mathbf{p}, t)}{\partial t} = -\frac{\partial[\dot{p}_i\psi(\mathbf{p}, t)]}{\partial p_i} \tag{8}$$

The solution of Eq. (8) provides the complete information on the fiber orientation state. However, to solve Eq. (8), proper expression for $\dot{p}_i$ should be used.

SOLUTION FOR THE DISTRIBUTION FUNCTION

If the fibers are assumed to be initially random, then the initial condition for Eq. (8) can be obtained from normalization conditions given in Eq. (5) and Eq. (7). For planar orientations, the initial condition is given as:

$$\psi_\theta(\theta, t = 0) = \frac{1}{\pi} \tag{9}$$

and for three-dimensional orientations:

$$\psi(\phi, \theta, t = 0) = \frac{1}{4\pi} \tag{10}$$

By using Eq. (10) as the initial condition, and considering that Eq. (3) is used in Eq. (8), the solution for the distribution function is given as[5]

$$\psi(\mathbf{p}, t) = \frac{1}{4\pi}(\mathbf{\Delta}^+\mathbf{\Delta}:\mathbf{pp})^{-3/2} \tag{11}$$

Similarly, for two-dimensional descriptions:

$$\psi_\theta(\mathbf{p}, t) = \frac{1}{\pi}(\mathbf{\Delta}^+\mathbf{\Delta}:\mathbf{pp})^{-1} \tag{12}$$

where $\mathbf{\Delta}$ is the deformation gradient tensor ($^+$ implies its transpose), and defined as:

$$\Delta_{ij} = \frac{\partial x_i'}{\partial x_j} \tag{13}$$

in which x_i' is the position vector at $t = 0$ and x_j is the position vector at time t. The deformation gradient for any homogeneous flow field can be expressed in terms of flow kinematics which makes the calculation of distribution function much easier.

Two-Dimensional Distribution Function

For any two-dimensional homogeneous flow field, the velocity gradient tensor can be specified as:

$$u_{i,j} = \begin{pmatrix} c & c_1 \\ c_2 & -c \end{pmatrix} \tag{14}$$

where the trace of $u_{i,j}$ should be zero in order to satisfy the continuity equation, and c, c_1, c_2 are completely arbitrary constants.

The displacement field can be described by using $u_{i,j}$ and two first-order ordinary differential equations. This can be expressed as;

$$\frac{dx_1}{dt} = cx_1 + c_1x_2 \tag{15}$$

$$\frac{dx_2}{dt} = -cx_2 + c_2x_1 \tag{16}$$

with the initial conditions;

$$x_1 = x_1' \quad \text{and} \quad x_2 = x_2' \quad \text{at } t = 0$$

The solution of Eqs. (15) and (16) provides the deformation gradient tensor Δ_{ij} in terms of the components of the velocity gradient tensor $u_{i,j}$.

There are three different cases depending on the sign of the parameter $\omega_n^2 = c^2 + c_1c_2$.

$c^2 + c_1c_2 = 0$, i.g., shear flows:

$$\mathbf{\Delta} = \begin{pmatrix} 1 - ct & -c_1t \\ -c_2t & 1 + ct \end{pmatrix} \tag{17}$$

$c^2 + c_1c_2 > 0$, e.g., elongational flows:

$$\mathbf{\Delta} = \begin{pmatrix} \dfrac{\omega_n - c}{2\omega_n} e^{\omega_n t} + \dfrac{\omega_n + c}{2\omega_n} e^{-\omega_n t} & \dfrac{c_1}{2\omega_n} (e^{-\omega_n t} - e^{\omega_n t}) \\ \dfrac{c_2}{2\omega_n} (e^{-\omega_n t} - e^{\omega_n t}) & \dfrac{\omega_n - c}{2\omega_n} e^{-\omega_n t} + \dfrac{\omega_n + c}{2\omega_n} e^{\omega_{nt}} \end{pmatrix} \tag{18}$$

$c^2 + c_1c_2 < 0$, e.g., rotational flows:

$$\mathbf{\Delta} = \begin{pmatrix} \cos\sqrt{|\omega_n^2|}t - \dfrac{c}{\sqrt{|\omega_n^2|}} \sin\sqrt{|\omega_n^2|}t & -\dfrac{c_1}{\sqrt{|\omega_n^2|}} \sin\sqrt{|\omega_n^2|}t \\ -\dfrac{c_2}{\sqrt{|\omega_n^2|}} \sin|\omega_n^2|t & \cos\sqrt{|\omega_n^2|}t + \dfrac{c}{\sqrt{|\omega_n^2|}} \sin\sqrt{|\omega_n^2|}t \end{pmatrix} \tag{19}$$

The two-dimensional solution of distribution function can be explicitly written from Eq. (12) as:

$$\psi_\theta(\theta, t) = \frac{1}{\pi}[(\Delta_{11}^2 + \Delta_{21}^2)p_1^2 + (\Delta_{11}\Delta_{12} + \Delta_{21}\Delta_{22})2p_1 p_2 + (\Delta_{12}^2 + \Delta_{22}^2)p_2^2]^{-1} \quad (20)$$

where

$$\mathbf{p} = \begin{pmatrix} p_1 \\ p_2 \end{pmatrix} = \begin{pmatrix} \cos\theta \\ \sin\theta \end{pmatrix} \quad (21)$$

For simple shear flow, the velocity gradient tensor is specified as:

$$u_{i,j} = \begin{pmatrix} 0 & \gamma/t \\ 0 & 0 \end{pmatrix}; \qquad \omega_n^2 = 0 \quad (22)$$

where γ is the total shear. Therefore, the distribution function for simple shear flow is:

$$\psi_\theta(\theta, \gamma) = \frac{1}{\pi}[1 - \gamma \sin 2\theta + \gamma^2 \sin^2\theta]^{-1} \quad (23)$$

Similarly, for planar elongational flow,

$$u_{i,j} = \begin{pmatrix} \epsilon/t & 0 \\ 0 & -\epsilon/t \end{pmatrix}; \qquad \omega_n^2 > 0 \quad (24)$$

In this case ϵ is the total elongation, and the distribution function for planar elongational flow is:

$$\psi_\theta(\theta, \epsilon) = \frac{1}{\pi}[e^{-2\epsilon}\cos^2\theta + e^{2\epsilon}\sin^2\theta]^{-1} \quad (25)$$

The two-dimensional distribution function is calculated for simple shear flows from Eq. (23) at five different total shears, up to 1.25 and is shown in Figure 1.

Similarly, the two-dimensional distribution function for planar elongational flow is calculated by using Eq. (25). Figure 2 depicts the distribution function at five different total elongations starting with random orientation.

The preferred angle for fiber orientation for a given total shear can be calculated by considering:

$$\frac{\partial\psi(\theta, \gamma)}{\partial\theta} = 0 \quad (26)$$

which gives

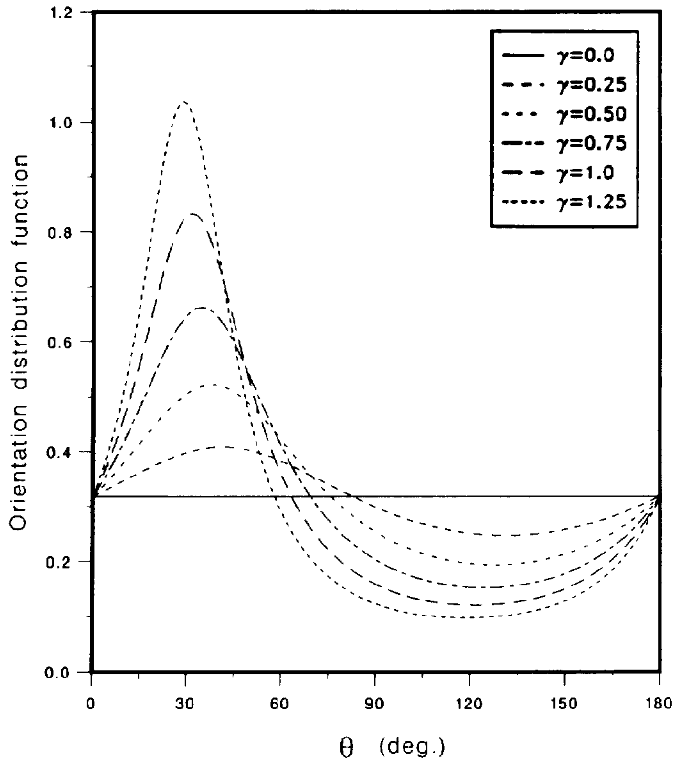

Fig. 1. Two-dimensional orientation distribution function in simple shear flow. θ is measured from the flow direction.

$$\theta = \frac{1}{2}\tan^{-1}(2/\gamma) \tag{27}$$

Figure 3 shows the preferred angle for fiber orientation versus total shear. A similar type of qualitative behavior for the preferred angle in simple shear flows is also observed in studies based on Doi's model which was developed for the polymeric liquid crystals.[20]

Three-Dimensional Distribution Function

For complete three-dimensional homogeneous flow fields, the same methodology can be used to describe the deformation gradient tensor. However, the manipulations are cumbersome. Therefore, in this work, special cases of three-dimensional homogeneous flow fields are considered. The flow between two paral-

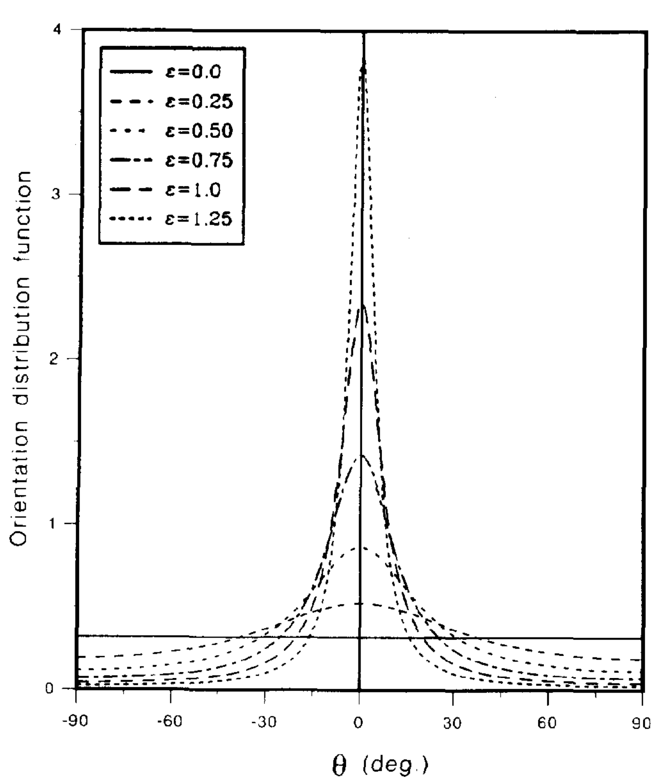

Fig. 2. Two-dimensional orientation distribution function in planar elongational flow. θ is measured from the flow direction.

lel plates separated by a small distance has only two velocity components. On the other hand, velocity gradients may exist in three different planes leading to a three-dimensional orientation. For these kinds of flow fields, the velocity gradient tensor is specified as:

$$u_{i,j} = \begin{pmatrix} c & c_1 & c_3 \\ c_2 & -c & c_4 \\ 0 & 0 & 0 \end{pmatrix} \tag{28}$$

The planar velocity components are now functions of the third direction, through c_3 and c_4. These types of flow fields are often encountered in injection molding processes. Such processes are usually modelled as flows between plates separated by a thin gap width. The velocity field of these complex flows are often solved by discretizing the domain. At each nodal point, c, c_1, and c_2 characterize the local planar velocity gradients and, c_3 and c_4 characterize the variation of velocity field through the gap thick-

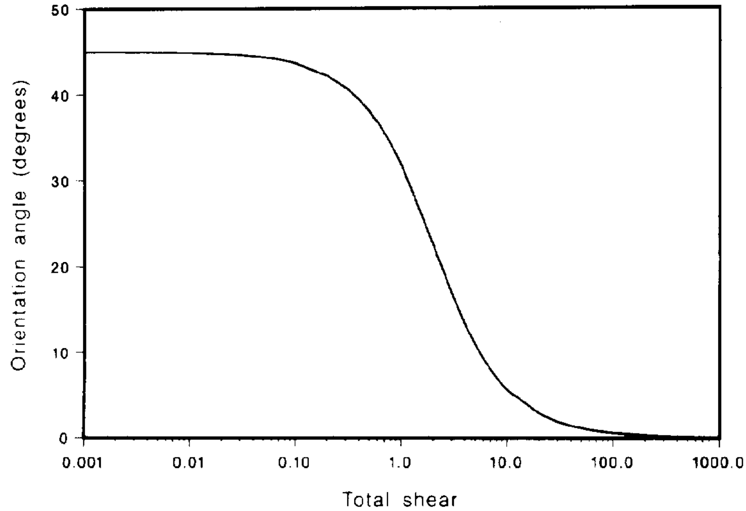

Fig. 3. Maximum orientation angle vs. total shear for simple shear flow.

ness. In order to predict the fiber orientation in complex flows, the distribution function needs to be solved several times along a particle path, and by considering the several local velocity gradient tensors. A similar solution by using Jeffery's equation is reported by Givler[21] and Jackson et al.[7] for two-dimensional flows.

For three-dimensional descriptions, the explicit expression for the distribution function can be written from Eq. (11) as:

$$\begin{aligned}\psi(\theta,\phi,t) = \frac{1}{4\pi}[&(\Delta_{11}^2 + \Delta_{21}^2 + \Delta_{31}^2)p_1^2\\ &+ (\Delta_{11}\Delta_{12} + \Delta_{21}\Delta_{22} + \Delta_{31}\Delta_{32})2p_1p_2\\ &+ (\Delta_{11}\Delta_{13} + \Delta_{21}\Delta_{23} + \Delta_{31}\Delta_{33})2p_1p_3\\ &+ (\Delta_{12}^2 + \Delta_{22}^2 + \Delta_{32}^2)p_2^2\\ &+ (\Delta_{12}\Delta_{13} + \Delta_{22}\Delta_{23} + \Delta_{32}\Delta_{33})2p_2p_3\\ &+ (\Delta_{13}^2 + \Delta_{23}^2 + \Delta_{33}^2)p_3^2]^{-3/2}\end{aligned} \tag{29}$$

where

$$\mathbf{p} = \begin{pmatrix} p_1 \\ p_2 \\ p_3 \end{pmatrix} = \begin{pmatrix} \sin\theta\cos\phi \\ \sin\theta\sin\phi \\ \cos\theta \end{pmatrix} \tag{30}$$

From the given velocity gradient tensor $u_{i,j}$, the resulting two ordinary nonhomogeneous differential equations can be obtained as

$$\frac{dx_1}{dt} - cx_1 - c_1x_2 = c_3x_3' \qquad (31)$$

$$\frac{dx_2}{dt} - c_2x_1 + cx_2 = c_4x_3' \qquad (32)$$

with the initial conditions:

$$x_1 = x_1' \quad \text{and} \quad x_2 = x_2' \quad \text{at } t = 0$$

Following the same procedure as in two-dimensional case, Eq. (31) and Eq. (32) are solved to obtain the deformation gradient tensor Δ_{ij}.

$$\Delta_{ij} = \begin{pmatrix} (\Delta_{11})_{2D} & (\Delta_{12})_{2D} & \Delta_{13} \\ (\Delta_{21})_{2D} & (\Delta_{22})_{2D} & \Delta_{23} \\ 0 & 0 & 1 \end{pmatrix} \qquad (33)$$

where
For $c^2 + c_1c_2 = 0$:

$$\Delta_{13} = \frac{1}{2}(cc_3 + c_1c_4)t^2 - c_3t \qquad (34)$$

$$\Delta_{23} = \frac{1}{2}(c_2c_3 - cc_4)t^2 - c_4t \qquad (35)$$

For $c^2 + c_1c_2 > 0$:

$$\Delta_{13} = \left(\frac{c_1c_4 + cc_3}{2\omega_n^2} - \frac{c_3}{2\omega_n}\right)e^{\omega_n t} + \left(\frac{c_1c_4 + cc_3}{2\omega_n^2} + \frac{c_3}{2\omega_n}\right)e^{-\omega_n t} - \left(\frac{c_1c_4 + cc_3}{\omega_n^2}\right) \qquad (36)$$

(37)

$$\Delta_{23} = \left(\frac{c_2c_3 + cc_4}{2\omega_n^2} - \frac{c_4}{2\omega_n}\right)e^{\omega_n t} + \left(\frac{c_2c_3 - cc_4}{2\omega_n^2} + \frac{c_4}{2\omega_n}\right)e^{-\omega_n t} - \left(\frac{c_2c_3 + cc_4}{\omega_n^2}\right) \qquad (38)$$

For $c^2 + c_1c_2 < 0$:

$$\Delta_{13} = \frac{c_1c_4 + cc_3}{\omega_n^2}(\cos\sqrt{|\omega_n^2|}t) - \frac{c_3}{\omega_n}\sin\sqrt{|\omega_n^2|}t \qquad (39)$$

$$\Delta_{23} = \frac{c_2c_3 + cc_4}{\omega_n^2}(\cos\sqrt{|\omega_n^2|}t) - \frac{c_4}{\omega_n}\sin\sqrt{|\omega_n^2|}t \qquad (40)$$

The other components of the deformation gradient tensor remain the same as in the two-dimensional solution.

One important flow types in polymer processing is the uniaxial extensional flow, which often occur in blow molding, spinning, and foaming operations. The velocity gradient tensor for this type of flows is:

$$u_{i,j} = \begin{pmatrix} \epsilon/t & 0 & 0 \\ 0 & -\epsilon/2t & 0 \\ 0 & 0 & -\epsilon/2t \end{pmatrix} \tag{41}$$

Therefore, the deformation gradient tensor $\mathbf{\Delta}_{ij}$ becomes:

$$\mathbf{\Delta}_{ij} = \begin{pmatrix} e^{-\epsilon} & 0 & 0 \\ 0 & e^{\epsilon/2} & 0 \\ 0 & 0 & e^{\epsilon/2} \end{pmatrix} \tag{42}$$

Using Eq. (42) together with Eq. (29) and Eq. (30), the explicit expression for distribution function is obtained as:

$$\psi(\theta, \phi, \epsilon) = \frac{1}{4\pi}[e^{-2\epsilon} \sin^2\theta \cos^2\phi + e^{\epsilon} \sin^2\theta \sin^2\phi + e^{\epsilon} \cos^2\theta]^{-3/2} \tag{43}$$

These solutions of the orientation distribution function provide the complete transient information about the fiber orientation state for the flows under consideration. Despite being the most accurate, this approach for describing the fiber orientation is not convenient for three-dimensional cases. In the next section, the possibility of presenting the same information with orientation tensors is investigated.

ORIENTATION TENSORS

Orientation tensors are a suitable and concise way of describing the orientation state.[4] Since the distribution function is even, only even-order tensors describe the orientation state. The second- and fourth-order orientation tensors are defined as:

$$S_{ij} \equiv \langle p_i p_j \rangle \equiv \oint p_i p_j \psi(\mathbf{p})\, d\mathbf{p} \tag{44}$$

$$S_{ijkl} \equiv \langle p_i p_j p_k p_l \rangle \equiv \oint p_i p_j p_k p_l \psi(\mathbf{p})\, d\mathbf{p} \tag{45}$$

These tensors represent the moments of distribution function, and are invariant under orthogonal transformations. They can be used for both two- and three-dimensional descriptions. The order of the indices is not important due to complete symmetry of these tensors. The normalization condition implies that the trace of the second-order orientation tensor is unity. Using these properties of the orientation tensors, one can easily show that the higher-order tensors contain the lower-order ones. Therefore, the total number of independent components of an nth-order tensor is:

$$N = \sum_{i=1}^{n/2} (4i + 1) \tag{46}$$

The non-zero second-order tensor components are calculated for simple shear and planar elongational flows by using Eq. (23) and Eq. (25) together with Eq. (44). The IMSL integration subroutine DBLIN,[22] which utilizes the adaptive Romberg method, is used and the results are shown in Figures 4 and 5. From the components of second-order tensor, orientation state can be described using ellipsoids. The eigenvalues and the eigenvectors of the second-order orientation tensor give the three major axes of the ellipsoid, and indicate the degree of orientation along these directions. The orientation ellipsoids are calculated for two different total shear and total elongation, and the three orthogonal views of the orientation ellipsoids are shown in Figures 6 and 7.

The rheological properties of the fiber suspensions can be easily calculated with the fourth-order tensor $\mathbf{S}_{ijkl}$ using the Dihn-Armstrong model. For shear flows, the transient viscosity, first

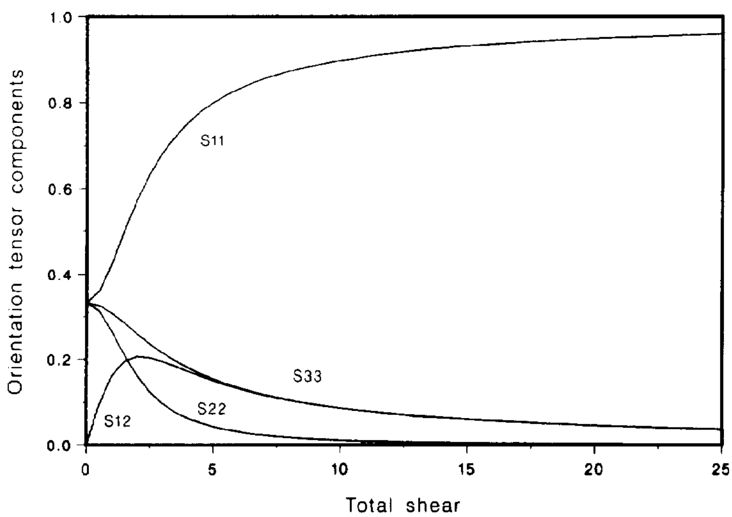

Fig. 4. Non-zero components of second-order orientation tensor for simple shear flow.

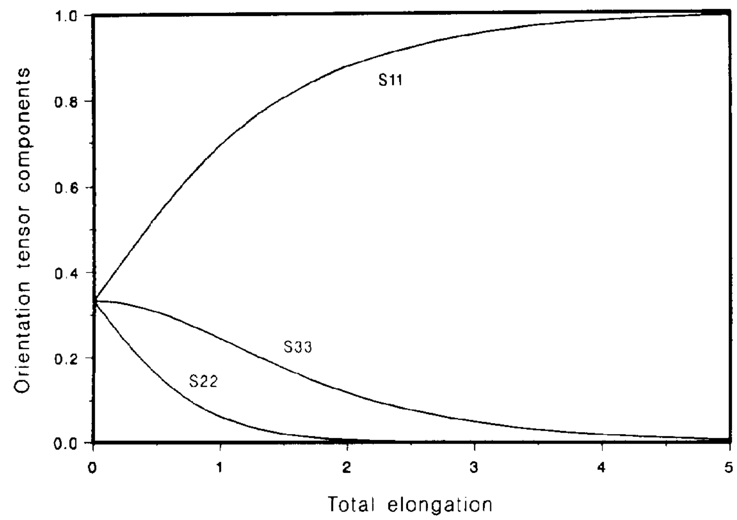

Fig. 5. Non-zero components of second-order orientation tensor for planar elongational flow.

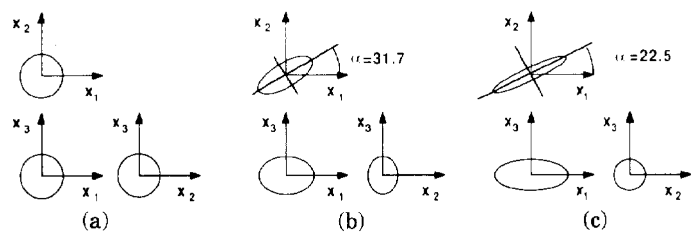

Fig. 6. Orientation ellipsoids for simple shear flow: (a) $\gamma = 0.0$; (b) $\gamma = 1.0$; (c) $\gamma = 2.0$.

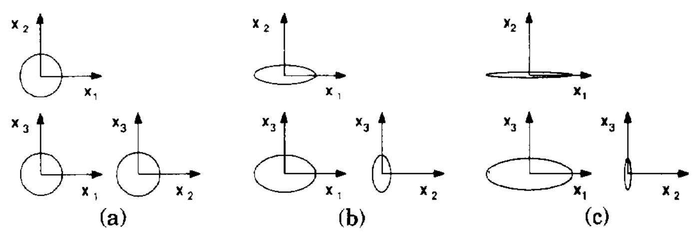

Fig. 7. Orientation ellipsoids for planar elongational flow: (a) $\epsilon = 0.0$; (b) $\epsilon = 0.5$; (c) $\epsilon = 1.0$.

normal stress difference, and the second normal stress difference are used to characterize the behavior of fiber suspensions. These quantities are defined as:

$$\mu^+ = \sigma_{12}/\dot{\gamma} \tag{47}$$

$$\Psi_1^+ = (\sigma_{11} - \sigma_{22})/\dot{\gamma}^2 \tag{48}$$

$$\Psi_2^+ = (\sigma_{22} - \sigma_{33})/\dot{\gamma}^2 \tag{49}$$

Similarly, for planar elongational flow, the planar extensional viscosity is defined as:

$$\mu_p^+ = (\sigma_{11} - \sigma_{22})/\dot{\epsilon} \tag{50}$$

In order to characterize the rheological properties, the dimensionless parameters for fiber suspensions are obtained from Eq. (2).

$$\left[\frac{\mu^+}{\mu} - 1\right]\frac{6\ln\left(\frac{2H}{d}\right)}{\pi l^3 n} = S_{1122} \tag{51}$$

$$\Psi_1^+\frac{6\ln\left(\frac{2H}{d}\right)\dot{\gamma}}{\mu\pi l^3 n} = S_{1112} - S_{1222} \tag{52}$$

$$\Psi_2^+\frac{6\ln\left(\frac{2H}{d}\right)\dot{\gamma}}{\mu\pi l^3 n} = S_{1222} - S_{1233} \tag{53}$$

$$\left[\frac{\mu_p^+}{\mu} - 4\right]\frac{6\ln\left(\frac{2H}{d}\right)}{\pi l^3 n} = S_{1111} + S_{2222} - 2S_{1122} \tag{54}$$

These expressions show that the rheological properties can be directly obtained from the fourth-order orientation tensor components.

Instead of calculating the distribution function and then determining the orientation tensors, the time evolution of the orientation tensors, i.e., $\mathbf{S}_{ij}$, can be expressed in terms of the flow kinematics by suitable integration of the Fokker–Plank equation. However, the resulting expression always generates a classic closure problem; that is, the expression contains the next even higher-order orientation tensor, i.e., $\mathbf{S}_{ijkl}$, which is not known. This problem also emerges in several other areas of rheology as well as in many other stochastic systems. Usually, a closure approximation is used where the higher-order tensor is expressed in terms of the lower-order ones. This reduces the problem to a closed set of equations. The form of closure approximations affects both the accuracy of the description of the orientation state (maximum orientation angle and the degree of alignment) and the predictions of the stresses generated due to fibers. Therefore, the investigation of the order and the type of closure approximations is needed for the accurate and efficient characterization of the suspension behavior. The simplest and widely used ones are quadratic (preaveraging),[23,24]

$$S_{ijkl} = S_{ij}S_{kl} \tag{55}$$

and linear (first order),[16–18]

$$S_{ijkl} = -\frac{1}{35}(\delta_{ij}\delta_{kl} + \delta_{ik}\delta_{jl} + \delta_{il}\delta_{jk}) + \frac{1}{7}(S_{ij}\delta_{kl} + S_{ik}\delta_{jl} + S_{kl}\delta_{ij} + S_{jl}\delta_{ik} + S_{jk}\delta_{il} + S_{il}\delta_{jk}) \tag{56}$$

approximations. Particularly, in process simulations the *ad hoc* quadratic approximation is used most often. Although the quadratic approximation introduces nonlinearity into the system, the solution is relatively easy to obtain and the results are always stable. On the other hand, this approximation does not preserve required tensorial symmetry; that is, the two components of the orientation which are defined to be equivalent can be approximated in two different ways (i.e., $S_{1122} \simeq S_{11}S_{22}$ and $S_{1212} \simeq S_{12}^2$). The linear approximation yields satisfactory results when the fibers are relatively random. In fact, one can show that the linear closure is exact for the completely random orientation states. For shear flows, this approximation is successfully applied to dilute systems for smaller fiber aspect ratios, (i.e., $a_p < 10$). However, the error actually depends on the a_p, and the closure equation fails completely as $a_p \to \infty$ (either diverges or oscillates).[25] These observations are also confirmed in the study of Advani and Tucker[4] for planar orientations. Consequently, the implementation of linear closure is ruled out for the Dinh-Armstrong model, which utilizes the Jefferys equation with infinite aspect ratio. Nevertheless, another alternative is to use a hybrid scheme which combines the quadratic and linear approximations with a parameter f. This composite approximation can perform more accurately and stably over the entire range of orientation states with the proper choice of f.[4]

$$S_{ijkl} = (1 - f)S_{ijlk_{LINEAR}} + fS_{ijkl_{QUADRATIC}} \tag{57}$$

Here, the parameter f must be a function of the invariants of the orientation tensor and must be unity when all fibers are aligned and must vanish when all fibers are random. For three-dimensional flows, among several other choices, f is taken as:[26]

$$f = 1 - 27I_3 \tag{58}$$

$$I_3 = \frac{1}{6}(1 - 3S_{ij}S_{ji} + 2S_{ij}S_{jk}S_{ki}) \tag{59}$$

For simple shear and planar elongational flows, the exact fourth-order orientation tensor components are calculated by using Eqs. (29) and (30) together with Eq. (45). Again, IMSL integration subroutine DBLIN is used. Some of the non-zero fourth-order components are also estimated from the exact second-order components with quadratic and hybrid approximation, and are compared with the exact results calculated from Eq. (45). These are shown in Figures 8 and 9.

The exact and approximated results for the dimensionless transient viscosity S_{1122} are shown in Figure 8(c). The other rheological properties given in Eqs. (57)–(59) are calculated from the exact results and are also estimated with quadratic and hybrid approximations. These are depicted in Figures 10 to 12.

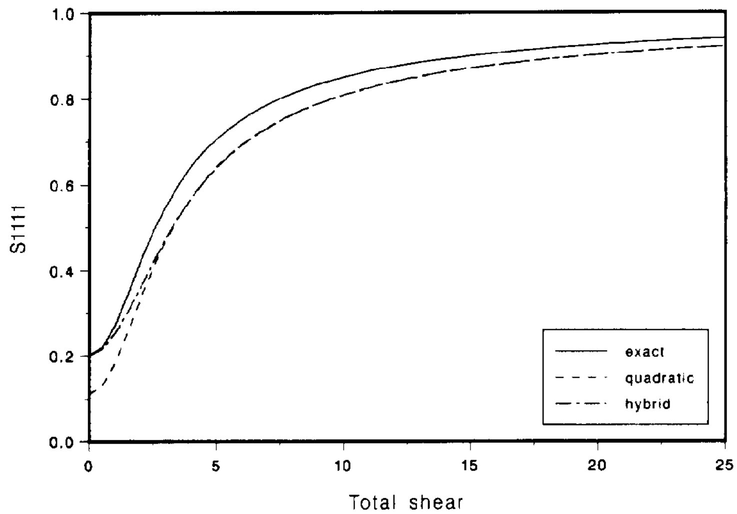

(a)

Fig. 8. Approximations for the fourth-order orientation tensor components vs. total shear for simple shear flow. (a) S_{1111}; (b) S_{3333}; (c) S_{1122}; (d) S_{1133}. ——, exact; - - -·, quadratic; — — —, hybrid.

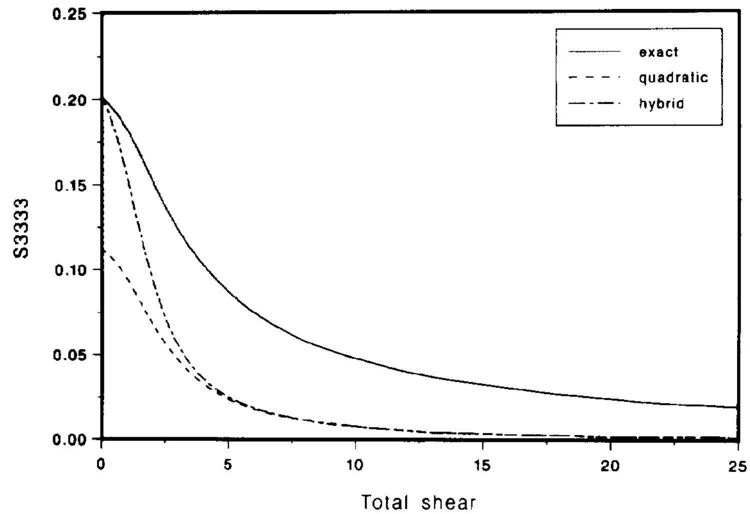

(b)

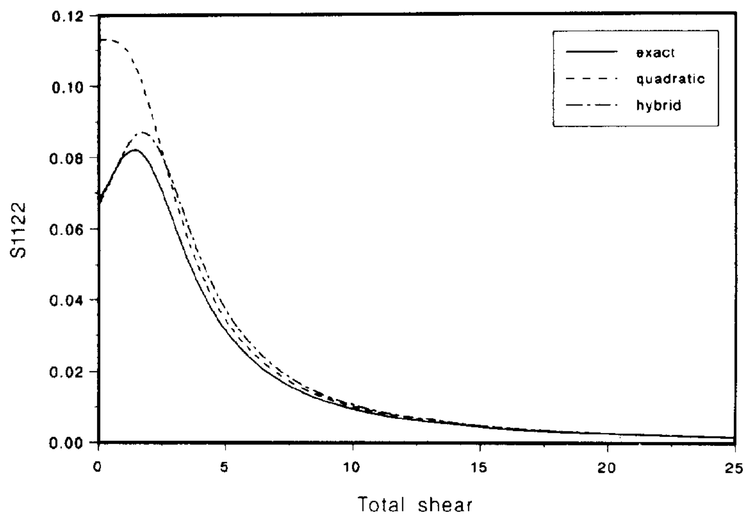

(c)

(Fig. 8. continued)

RESULTS AND DISCUSSION

In this work, the solutions of the two-dimensional and three-dimensional orientation distribution function are obtained in

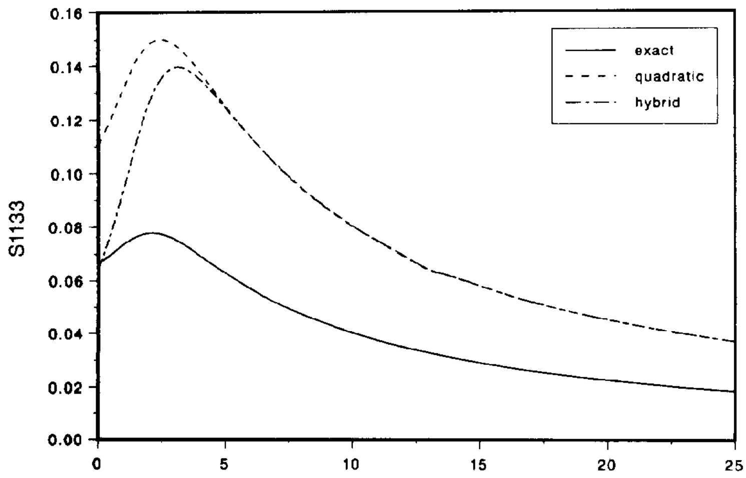

(d)

(Fig. 8. continued)

terms of the velocity gradients. The governing equation for the orientation distribution function is based on the Dinh-Armstrong model for semiconcentrated fiber suspensions.

The two-dimensional distribution function is calculated for simple shear and planar elongational flows by using random initial conditions. Figures 1 and 2 show that once the shear rate or elongational rate is specified, the governing parameter for the orientation is total shear or total elongation. These figures clearly indicate that the elongational flow is much more effective in aligning the fibers. The results for the simple shear flow show that the alignment of fibers starts around 45 degrees with flow direction for very small total shears, and as the total shear increases, fibers tend to align in the shear direction. At high total shears, the distribution function narrows down, indicating that the fibers are more likely to be around the preferred angle. Figure 3 shows the preferred angle versus total shear. This maximum angle of orientation starts at 45 degrees and asymptotically approaches zero at infinitely high total shears. For planar elongational flows, the fibers are always most likely to be around the elongation axis.

Although similar qualitative behavior is observed in Doi's model, the maximum orientation angle starts at different values (lower than 45 degrees) for zero shear limit depending on a dimensionless concentration coefficient U. The initial orienta-

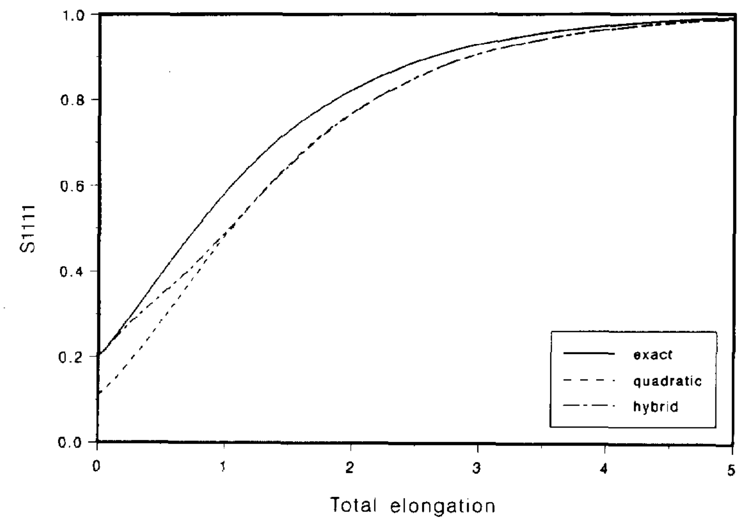

(a)

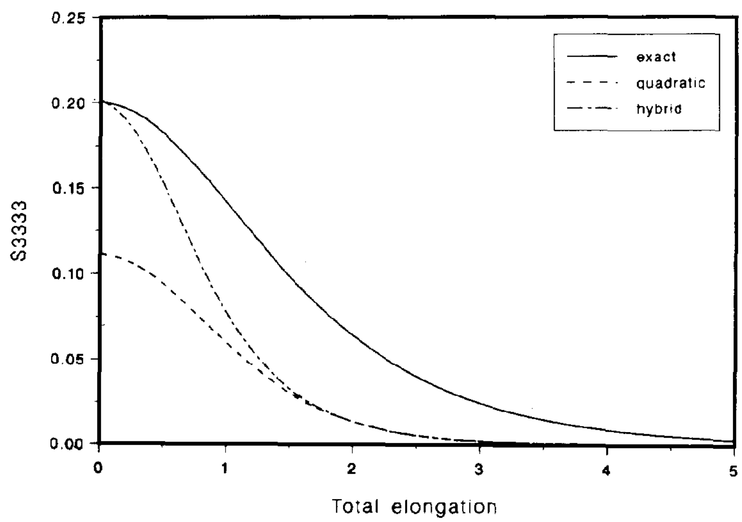

(b)

Fig. 9. Approximations for the fourth-order orientation tensor components vs. total elongation for planar elongational flow. (a) S_{1111}; (b) S_{3333}; (c) S_{1133}. ——, exact; - - - ·, quadratic; — — — —, hybrid.

tion angle is predicted to be decreasing with the increase in concentration. On the other hand, Doi's model also predicts perfect alignment with the flow at infinitely high total shears but the rate of alignment is predicted to be at a much slower rate com-

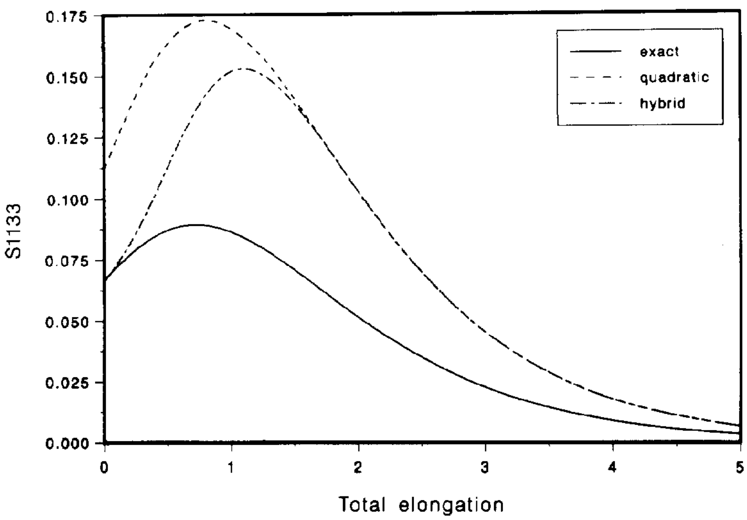

(c)

(Fig. 9. continued)

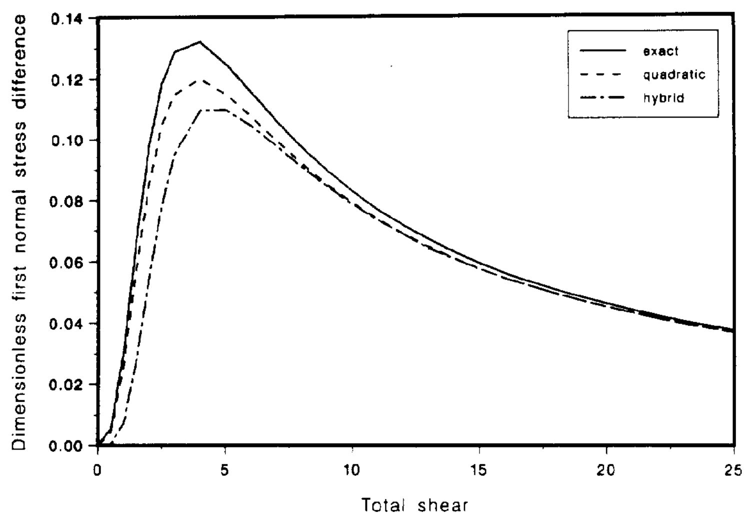

Fig. 10. Approximated dimensionless first normal stress difference vs. total shear for simple shear flow. ——, exact; – – –, quadratic; — — —, hybrid.

pared with the Dinh-Armstrong model.[20] Another similarity between these two models is that the orientation state is a function of the total strain (i.e., total shear, total elongation) not the strain rate or time separately.[27]

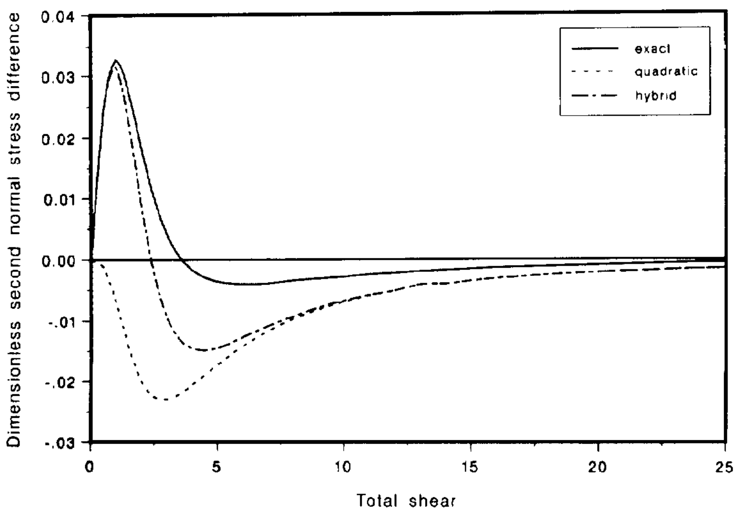

Fig. 11. Approximated dimensionless second normal stress difference vs. total shear for simple shear flow. ——, exact; – – –, quadratic; — - —, hybrid.

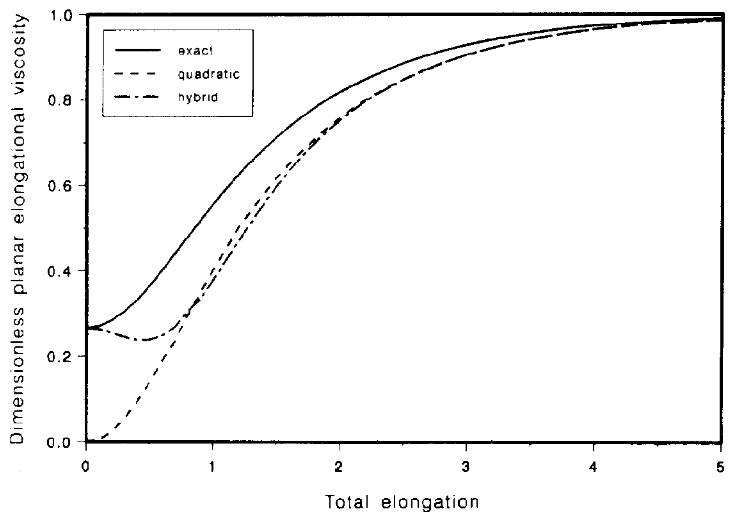

Fig. 12. Approximated dimensionless planar elongational viscosity vs. total elongation for planar elongational flow. ——, exact; – – –, quadratic; — - —, hybrid.

The analytical solutions are then employed to calculate the orientation tensor components, which can be used to approximate the fiber orientation state. For simple shear flows, the nonzero components of the second-order orientation tensor are calculated up to total shear of 25 and are shown in Figure 4.

S_{11} is the second moment of distribution function with respect to flow direction. Similarly, S_{33} is calculated with respect to the X_3 direction (neutral axis). Since $S_{11} + S_{22} + S_{33} = 1$, only two of the diagonal components of this tensor are independent. Therefore, together with S_{12}, there are three independent non-zero components. The non-zero S_{12} indicates a preferred direction that does not coincide with the coordinate axes used in the flow description. In Figure 4, S_{11} approaches 1 asymptotically, and all the other components go to zero at very high total shear, which indicates that all the fibers are aligned in the flow direction.

For planar elongational flows, the second-order tensor components are shown in Figure 5 up to a total elongation of 5. There are only two independent non-zero components. S_{11} is the second moment of distribution function with respect to flow direction. Since S_{11} is always greater than S_{22} and S_{33}, and the tensor is always diagonal, flow direction is the angle of maximum orientation all the time. Furthermore, $S_{33} > S_{22}$ indicates that the probability of having fibers along neutral direction is greater than having fibers perpendicular to the flow direction.

From the second-order tensor components, the orientation ellipsoid is used to decribe orientation state. For any second-order orientation tensor, three eigenvalues $\lambda_1 > \lambda_2 > \lambda_3$ and corresponding three eigenvectors $\mathbf{e}_1$, $\mathbf{e}_2$, and $\mathbf{e}_3$ can be found. The maximum orientation direction is specified by $\mathbf{e}_1$ and the degree of orientation along that direction is governed by λ_1. The description of orientation state on any plane can be represented by the projection of the orientation ellipsoid on that plane. The graphical representations of three-dimensional fiber orientation for simple shear and planar elongational flows are shown in Figures 6 and 7. Since the initial orientation distribution is described by a sphere, all three views of the distribution function are shown as circles with radius $1/4\pi$. In these figures, x_1 is the flow direction and x_3 is the neutral axis. For shear flow, the preferred angle is always in the shear plane. Neither flow has axisymmetric orientation distribution. As shown in Figures 6 and 7, the orientation ellipsoids are deformed faster in the shear and extensional x_1–x_2 plane in comparison with the neutral x_1–x_3 plane.

The fourth-order tensor components are approximated using quadratic and hybrid approximation from the exact values of second-order tensor. As Eqs. (56)–(59) indicate, the rheological properties which are commonly used in the characterization of fluids can be expressed in terms of the fourth-order tensor. In fact, each independent component of the fourth-order tensor is related directly to the rheology of the fiber suspensions. Although approximating the fourth-order tensor from second-order tensor has been widely used, these approximations can introduce significant errors in stress states as well as orientation descriptions.

The approximations for some non-zero fourth-order tensor components for simple shear flow are shown in Figure 8(a)–(d). In Figure 8(b) and 8(d), the quantitative discrepancy is quite large. For planar elongational flow, the approximations for some non-zero fourth-order orientation tensor components are shown in Figure 9(a)–(d). In this case, Figure 9(b) and 9(d) have considerable quantitative errors.

In rheological predictions for simple shear flow, the approximations for transient viscosity agreed well with the exact value, except the quadratic closure started at a different value at the zero strain limit, but converged quickly to the exact solution. Both approximations performed well for the first normal stress difference; however, for the second normal stress difference, quadratic closure failed to depict the initial overshoot and both closures exhibit large undershoots, resulting in considerable inaccuracy. For planar elongational viscosity, approximate solutions are in qualitative agreement but quantitative accuracy was not satisfactory for small strains (i.e., for $\epsilon < 1$).

Since all of the independent non-zero components of the fourth-order orientation tensor are needed to describe the rheology of the suspension, the type and the order of approximations used needs to be examined thoroughly. The approximations may result in even larger errors for complex flow fields, where both shear and elongational velocity gradients exist in all three different planes. Therefore, higher-order approximations may be required for the accurate description of suspension mechanics.

CONCLUDING REMARKS

In this study, the two- and three-dimensional description of fiber orientation is presented for arbitrary homogeneous flows. The equation of motion of fibers is based on the Dinh-Armstrong model. The solution for orientation distribution function is expressed in terms of fluid kinematics, which permits accurate calculation of the orientation tensor components. From second-order orientation tensor components, an orientation ellipsoid is defined to represent the three-dimensional orientation state of the fiber suspensions.

The analysis showed that the commonly used rheological properties for these material systems can be expressed as the combinations of fourth-order orientation tensor components. The fourth-order tensor components are estimated from the exact second-order components through hybrid and quadratic approximations. Usually, the hybrid approximation gave better results. This approximation always started from the exact value; however, in most cases, it quickly converged to the quadratic approximation.

Although the exact and approximated fourth-order tensor components showed the same qualitative behavior, large quantitative discrepancies are observed in some cases, leading to inaccurate predictions of rheological properties.

This study was supported by the Center for Composite Materials through the National Science Foundation Engineering Research Centers program. The authors would like to thank Dr. A. N. Beris for his helpful discussions.

References

1. G. B. Jeffery, *Proc. Roy. Soc.*, **A102**, 161 (1922).
2. R. C. Givler, M. J. Crochet, and R. B. Pipes, *J. Compos. Mat.*, **17**, 330 (1983).
3. F. P. Folgar and C. L. Tucker, *J. Reinf. Plast. Compos.*, **3**, 98 (1984).
4. S. G. Advani and C. L. Tucker, *J. Rheol.*, **31**, 751 (1987).
5. S. M. Dinh and R. C. Armstrong, *J. Rheol.*, **28**, 207 (1984).
6. M. A. Bibbo, S. M. Dinh, and R. C. Armstrong, *J. Rheol.*, **29**, 905 (1985).
7. W. C. Jackson, S. G. Advani, and C. L. Tucker, *J. Compos. Mat.*, **20**, 539 (1986).
8. L. G. Leal and E. J. Hinch, *J. Fluid Mech.*, **46**, 685 (1971).
9. A. Okagawa, R. G. Cox, and S. G. Mason, *J. Coll. Int. Sci.*, **45**, 303 (1973).
10. S. R. Strand, S. Kim, and S. J. Karila, *J. Non-Newtonian Fluid Mech.*, **24**, 311 (1987).
11. S. G. Advani and C. L. Tucker, SPE Tech. pap., **34**, 687 (1988).
12. J. C. Seferis and R. L. McCullough, *Polym. Eng. Sci.*, **16**, 334 (1976).
13. M. Doi and S. F. Edwards, *J. Chem. Soc. Faraday Trans. II*, **74**, 560 (1978).
14. M. Doi and S. F. Edwards, *J. Chem. Soc. Faraday Trans. II*, **74**, 918 (1978).
15. J. G. Evans, Ph.D. dissertation, Cambridge University, Cambridge, 1975.
16. G. L. Hand, *J. Fluid Mech.*, **13**, 33 (1962).
17. E. J. Hinch and L. G. Leal, *J. Fluid Mech.*, **71**, 481 (1975).
18. E. J. Hinch and L. G. Leal, *J. Fluid Mech.*, **76**, 187 (1976).
19. G. K. Batchelor, *J. Fluid Mech.*, **46**, 813 (1971).
20. B. J. Edwards and A. N. Berris, *J. Rheol.*, **33**, 537 (1989).
21. R. C. Givler, Ph.D. dissertation, University of Delaware, Newark, DE, 1985.
22. C. deBoor, *Mathematical Software*, J. R. Rice, ed., Academic Press, New York, 1971.
23. G. G. Lipscomb, M. M. Denn, D. U. Hur, and D. V. Boger, *J. Non-Newtonian Fluid Mech.*, **26**, 297 (1988).
24. M. Doi, *J. Polym. Sci., Polym. Phys. Ed.*, **19**, 229 (1981).
25. P. L. Frattini and G. G. Fuller, *J. Fluid. Mech.*, **168**, 119 (1986).

26. S. G. Advani, Ph.D. dissertation, University of Illinois, Urbana-Champaign, IL, 1987.
27. D. Doraiswamy, Ph.D. dissertation, University of Delaware, Newark, DE, 1987.

Received October 26, 1988
Accepted February 22, 1989